A Murine Skeletal Adaptation That Significantly Increases Cortical Bone Mechanical Properties

Implications for Human Skeletal Fragility

Jeffrey Bonadio,* Karl J. Jepsen,‡ Monique K. Mansoura,‡ Rudolf Jaenisch,§ Janet L. Kuhn,‡ and Steven A. Goldstein‡

**Department of Pathology and the ‡Orthopaedic Research Laboratories, Section of Orthopaedic Surgery, University of Michigan, Ann Arbor, Michigan 48109-0650; §Department of Biology, Whitehead Institute for Biomedical Research, Massachusetts Institute of Technology, Cambridge, Massachusetts 02142*

Abstract

Mov13 mice carry a provirus that prevents transcription initiation of the α1(I) collagen gene. Mutant mice homozygous for the null mutation produce no type I collagen and die at mid-gestation, whereas heterozygotes survive to adulthood. Dermal fibroblasts from heterozygous mice produce ~ 50% less type I collagen than normal littermates, and the partial deficiency in collagen production results in a phenotype similar to osteogenesis imperfecta type I (an inherited form of skeletal fragility). In this study, we have identified an adaptation of Mov13 skeletal tissue that significantly improves the bending strength of long bone. The adaptive response occurred over a 2-mo period, during which time a small number of newly proliferated osteogenic cells produced a significant amount of matrix components and thus generated new bone along periosteal surfaces. New bone deposition resulted in a measurable increase in cross-sectional geometry which, in turn, led to a dramatic increase in long bone bending strength. (*J. Clin. Invest.* 1993. 92:1697–1705.) Key words: Genetics • biomechanics • Mov13 transgenic mice • osteogenesis imperfecta type I • osteoporosis

Introduction

Bone is a living composite material. There are estimates that normal bone is subject to an average of 1×10^6 cyclic loads per year (1). The ability to withstand the transmission of mechanical loads reflects (*a*) the nature, amount, and organization of the normal mineral and protein constituents of bone; (*b*) the way in which these constituents interact during mechanical loading; and (*c*) the ability of bone cells to adapt these constituents to change (2). Type I collagen contributes to the load-bearing capacity of skeletal tissues by assembling into ordered fibrils that associate with plate-shaped crystals of carbonate apatite (3). However, the intrinsic and extrinsic mechanical forces generated during load transmission and the interactions that take place between the collagenous extracellular matrix and apatite mineral are not well understood. As such, our understanding of type I collagen's contribution to the mechanical function of the skeleton is incomplete. Precise understanding of this role is important, given the abundance of type I collagen in skeletal tissues and the fact that naturally occurring mutations in type I collagen genes lead to inherited connective tissue diseases, such as osteogenesis imperfecta, that are characterized by profound skeletal fragility (4).

To further examine type I collagen function during load transmission, we have altered collagen gene expression in transgenic mice. Central to this work is the Mov13 strain, which carries a provirus that completely prevents transcription initiation of the murine α1(I) collagen gene in all cells except embryonic odontoblasts and ~ 5% of embryonic osteoblasts (5–8). (Regarding the latter, α1(I) collagen mRNA from the mutant allele is expressed only for a short period of time before the onset of retroviral gene transcription. Virus transcription, which is initiated at about day 16 of development, appears to effectively extinguish any further α1(I) collagen transcription.) Mice homozygous for the null mutation produce no type I collagen and die at mid-gestation (9), whereas heterozygotes survive to young adulthood. Dermal fibroblasts from heterozygous mice produce ~ 50% less type I collagen than normal littermates (10, 11). The partial deficiency in gene expression results in a 50% decrease in tissue collagen content, progressive hearing loss, and alterations in the mechanical properties of long bone (11). The heterozygous Mov13 mouse therefore serves as a model of the human inherited connective tissue disease osteogenesis imperfecta type I (OI type I).[1]

Load-deformation curves from a previous study (11) indicated that the Mov13 mutation increases the brittleness and decreases the strength of long bone. However, a mixed population of specimens-taken from female animals at different ages-were evaluated, and this aspect of the study design may have contributed to the relatively large standard deviations that were observed. To better control for the potential effects of gender and age, we recently conducted a study that used male mice only and evaluated the mechanical properties, as defined in Table I, of femur specimens from animals at 8 and 15 wk of age (12). The study groups included a series of transgenic animals with one, two (i.e., normal), or three functioning α1(I) collagen genes. In agreement with previous results (11), long bone specimens from Mov13 mice were less able to plastically deform than wild-type littermate controls (i.e., the Mov13 specimens were significantly more brittle than normal). Furthermore, overexpression of an α1(I) collagen gene in Mov13 mice rescued the specific defect in plastic deformation. Thus, we have demonstrated a direct correlation between the number of functioning collagen genes and the ability of cortical bone to

Address correspondence to Dr. Jeffrey Bonadio, Department of Pathology, University of Michigan, MSRB I, Room 3510, 1150 West Medical Center Drive, Ann Arbor, MI 48109-0650.

Received for publication 6 October 1992 and in revised form 29 March 1993.

J. Clin. Invest.

0021-9738/93/10/1697/09 $2.00
Volume 92, October 1993, 1697–1705

1. *Abbreviations used in this paper:* OI type I, osteogenesis imperfecta type I; SEM, scanning electron microscopy.

Table I. Definition of Biomechanical Terms

(*a*) load-deformation curve—graphical representation of the load deformation results from a mechanical test.
(*b*) brittleness—generalized term referring to the decreased capacity of a structure to deform beyond yielding and prior to fracture.
(*c*) strength—a measure of the stress at which a material fails.
(*d*) plastic deformation—deformation of a structure associated with permanent changes in architecture.
(*e*) ductility—generalized term referring to the increased capacity of a structure to deform under a given load beyond yield and before failing.
(*f*) four-point bending tests to failure—destructive mechanical test designed to quantify mechanical (pre- and post-yield) behavior of a structure when subjected to four point bending.
(*g*) compliance—the inverse of stiffness; a measure of the amount of elastic deformation a structure undergoes when subjected to a given load.
(*h*) moments of inertia—a measure of the geometric resistance of a structure to loading.
(*i*) Young's modulus of elasticity—a measure of the amount of elastic strain a material undergoes given an applied stress.

plastically deform. Taken together, these results suggest that type I collagen contributes to the normal ductile behavior of bone tissue, a result that has important implications for the fatigue and the failure properties of vertebrate long bone.

In the course of this work, we identified a skeletal adaptation that results in an unexpected increase in the strength of Mov13 long bone. We demonstrate in this paper that the adaptation is mediated by cortical bone cells that synthesize, deposit, and mineralize a significant amount of new bone along periosteal surfaces. Moreover, the increase in cross-sectional geometry leads to a dramatic increase in mechanical integrity. This effect of the adaptive response may be explained by a well established relationship between the macroscopic structure of bone and its mechanical function.

Methods

Animals. Only male mice were used in this study. As determined by pathological examination at the time of death, Mov13 mice that developed retrovirus-induced leukemia (5) were excluded from study. Independent femur specimens were obtained from cohorts of Mov13 mice and (C57 BI/6) wild-type littermate controls at 8 and 15 wk of age.

Determination of the failure load properties in bending of whole cortical bone. Whole bone four-point bending tests to failure were conducted on a servo-hydraulic testing system at a constant displacement rate of 0.5 mm/s (11). The evaluation of failure load properties included a total of 10 independent femur specimens from (C57 BI/6) wild-type mice at 8 wk of age, 9 independent specimens from 8-wk-old Mov13 mice, 7 independent femur specimens from wild-type mice at 15 wk of age, and 5 independent specimens from 15-wk-old Mov13 mice. Statistical significance was determined by the Behrens–Fisher *t* test to adjust for unequal variance.

Micro-computed tomography. Micro-computed tomography was used to quantify the average area, moments of inertia (bending and principal), and shape of a 2–3 mm mid-diaphyseal region of wild type and Mov13 femur specimens. This tomography method generates high resolution ($\sim$ 20 μm), three-dimensional images from a series of two-dimensional x-ray projections (13, 14). The scan section for each femur was consistently located using the distal aspect of the third trochanter as a bony landmark. Only the mid-diaphysis was scanned because a preliminary study indicated that whole bone specimens consistently failed in this region under our four-point bending conditions (Jepsen, K. J., unpublished data). Since the bending tests were conducted in an anterior to posterior direction, tomographic specimens were oriented so the anterior surface faced the scanning source, making it possible to align the reconstruction axes and thus directly correlate mechanical and geometrical properties. Specimens were kept moist during the 20-min (average) scan period. Specimens were mounted so that the longitudinal axis of the diaphysis was parallel to the *z*-axis of the scan coordinate system. Since mouse femurs exhibit very little anterior or lateral curvature, the *x*–*y* planes of the tomographic images were reliable representations of mid-diaphyseal transverse sections.

The scan region was divided into 20-μm sections producing an average of 150 transverse sections for each femur. The images were thresholded to delineate each pixel as "bone" or "nonbone" in a manner as described (14). Areal properties were calculated for each transverse section and then averaged over the entire scan region. This approach appropriately accounted for any variance in areal properties along the diaphysis, but assumed geometrical uniformity. In support of the latter, the standard deviations of areal properties for each bone were at most 10% of the means. Finally, the cross-sectional shape was reconstructed by locating the endosteal and periosteal surfaces at 36 equiangle positions. To identify regions of bone deposition and resorption, the reconstructed two-dimensional images were superimposed relative to a geometric centroid and to the anatomical axes of a specimen.

Geometrical properties representing the entire scan region from each femur specimen were averaged for cohorts of independent wild-type and Mov13 specimens at 8 and 15 wk of age. These cohorts included all specimens taken to failure in four-point bending tests (the latter were scanned before mechanical testing) plus a small number of femur specimens whose mechanical properties were not tested. Thus, the evaluation included a total of 13 independent femur specimens from wild-type mice at 8 wk of age, 12 independent specimens from 8-wk-old Mov13 mice, 7 independent femur specimens from wild-type mice at 15 wk of age, and 6 independent specimens from 15-wk-old Mov13 mice. Statistical significance was determined by the Behrens–Fisher *t* test to adjust for unequal variance.

Northern blots. Poly (A^+) RNA was prepared from 15-wk wild-type and Mov13 femur specimens using the FastTrack kit (InVitrogen Corp., San Diego, CA). Northern blotting was performed as described (15). A 369-bp α1(I) collagen cDNA probe, encoding a portion of the triple helical domain (16), was generated by the PCR. A 500-bp avian cytoplasmic β-actin cDNA probe (17) was generated by the same method. Probes were radiolabeled by the random priming method as described (15).

Determination of lacunar density. Left and right femur specimens from 8-wk wild type and Mov13 mice were harvested immediately after death, cleaned of soft tissue, and fixed in 70% ethanol. A 6–7-mm region of the diaphysis from each specimen was prestained with osteochrome and embedded in methyl methacrylate. Serial transverse sections (120 μm) were prepared using a low speed diamond saw (Isomet Corp., Springfield, VA). For backscattered scanning electron microscopy (SEM), each section was ground to 65 μm, glued to plexiglas slides, polished using 1 μm diamond dust, and carbon coated. As an estimate of cell number, the number of lacunae per unit volume was estimated using stereological principles. Four independent estimates of lacunar number were made (from the anterior, posterior, medial, and lateral quadrants) and then averaged. Lacunar density was calculated according to a previously established formula,

$$Nv = n/[A2c + t)]$$

where, n is the number of lacunae per field of area, A; $2c$ is the out-of-plane length of lacunae; and t is the section thickness. Since the analysis

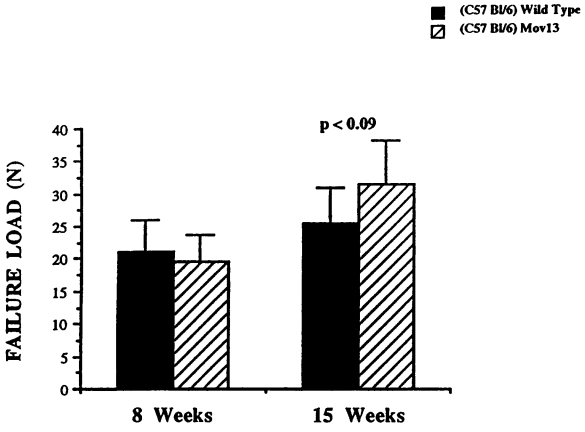

Figure 1. Bending strength of wild-type (C57 BI/6) and Mov13 mice. The analysis of failure load properties was performed as described in Methods.

was conducted using SEM, the section thickness, t, was essentially zero. The out-of-plane length of bone lacunae, $2c$, has been estimated as ~ 23.3 μm for human cortical bone (18) and was assumed to be a constant for both wild-type and Mov13 specimens. The evaluation included a total of five independent femur specimens from wild-type and Mov13 mice at 8 wk of age. Statistical significance was determined by an independent Student's t test assuming unequal variances.

Mineralization studies. Femurs of wild-type and Mov13 mice were retrieved after mechanical testing, and a 4–5 mm portion of the diaphysis was prepared. Marrow tissue was removed under a dissecting microscope by mechanical disruption. Specimens were degassed in water under a vacuum, returned to atmospheric pressure, and weighed in water while suspended from a fine wire. Specimens were centrifuged at 22°C for 15 min at 3,500 g to remove residual water and then reweighed to obtain the wet weight. Bone volume was determined using Archimede's principle (19). Specimens were ashed at 600°C for 18 h and then weighed. The following parameters were measured: bone density was calculated as the wet weight/bone volume; ash weight density was calculated as the ash weight/bone volume; and ash fraction was calculated as the ash weight density/bone density. Altogether, the evaluation included a total of four independent femur specimens from wild-type mice at 8 wk of age, four independent specimens from 8-wk-old Mov13 mice, four independent femur specimens from wild-type mice at 15 wk of age, and three independent specimens from 15-wk-old Mov13 mice. Statistical significance was evaluated by the Student's t test.

Results

The results of a companion study (12) indicated that the Mov13 mutation causes a general alteration in the mechanical integrity of cortical bone; i.e., relative to wild-type controls, the mutation was associated with a significant decrease in Young's modulus of elasticity, a measure of relative stiffness, as well as the post-yield deformation of whole bone specimens, a measure of relative plasticity or ductility (for both comparisons, $P < 0.004$). These results indicate that the Mov13 mutation leads to a decrease in long bone collagen content that, in turn, alters the structural and material properties of skeletal tissue.

On the basis of these results we predicted that the bending load to failure of Mov13 cortical bone, i.e., the amount of load required to break long bone specimens, would also be significantly decreased relative to wild-type controls. However, failure load values for wild-type and Mov13 femurs at 8 wk were not significantly different (Fig. 1). At 15 wk, Mov13 specimens actually showed a strong trend toward an increased failure load value relative to wild-type littermate controls ($P < 0.09$). Particularly striking was the fact that, relative to wild-type control values, the failure load properties of Mov13 femur specimens was increasing at the same time that other properties, such as the modulus of elasticity and postyield deformation, were decreasing.

The failure load value of long bone is strongly influenced by specimen geometry. We wondered, therefore, if the relative increase in the failure load value of 15-wk Mov13 femur specimens could be explained by a change in the geometry of the bending test site. Micro-computed tomography was used to quantify a 2–3 mm region near the mid-diaphysis. We found that the shape of wild-type and Mov13 specimens, as quantified by the ratio of principal moments of inertia (Iyy/Ixx), did not change significantly at 8 and 15 wk (compare values for the ratio of principal moments of inertia, Table II). Representative mid-diaphyseal transverse sections from a computer reconstruction of the digital data are shown in Fig. 2 *A*. We found only small differences in the cortical area of wild-type and Mov13 femur specimens at 8 wk (see also Table II). At 15 wk, however, the cortical area of Mov13 femur specimens was considerably increased relative to wild-type controls ($P < 0.003$). Schematic images of the sections shown in Fig. 2 *A* were prepared and superimposed in an effort to identify areas of cortical bone deposition and resorption. As shown in Fig. 2 *B*, the

Table II. Geometrical Properties (Shape) of (C57 BI/6) Wild-type and Mov13 Femur Specimens

Mouse	Age	Marrow cavity area	Cortical bone area	Bending moment of inertia	Ratio of principal moments of inertia
	wk	*mm²*	*mm²*	*mm²*	
C57 BI/6	8	1.05 (0.14)	0.73 (0.10)	0.128 (0.031)	0.516 (0.032)
Mov13	8	1.07 (0.15)	0.78 (0.09)	0.144 (0.032)	0.545 (0.047)
C57 BI/6	15	0.97 (0.09)	0.78 (0.11)	0.123 (0.036)	0.481 (0.063)
Mov13	15	1.09 (0.09)	1.01 (0.10)*§	0.200 (0.031)*§	0.549 (0.054)‡

Properties were calculated as described in Methods.
* Comparison between Mov13 and C57 BI/6, $P < 0.003$.
‡ Comparison between Mov13 and C57 BI/6, $P > 0.05$.
§ Comparison of Mov13 and 8- and 15 wk, $P < 0.005$.

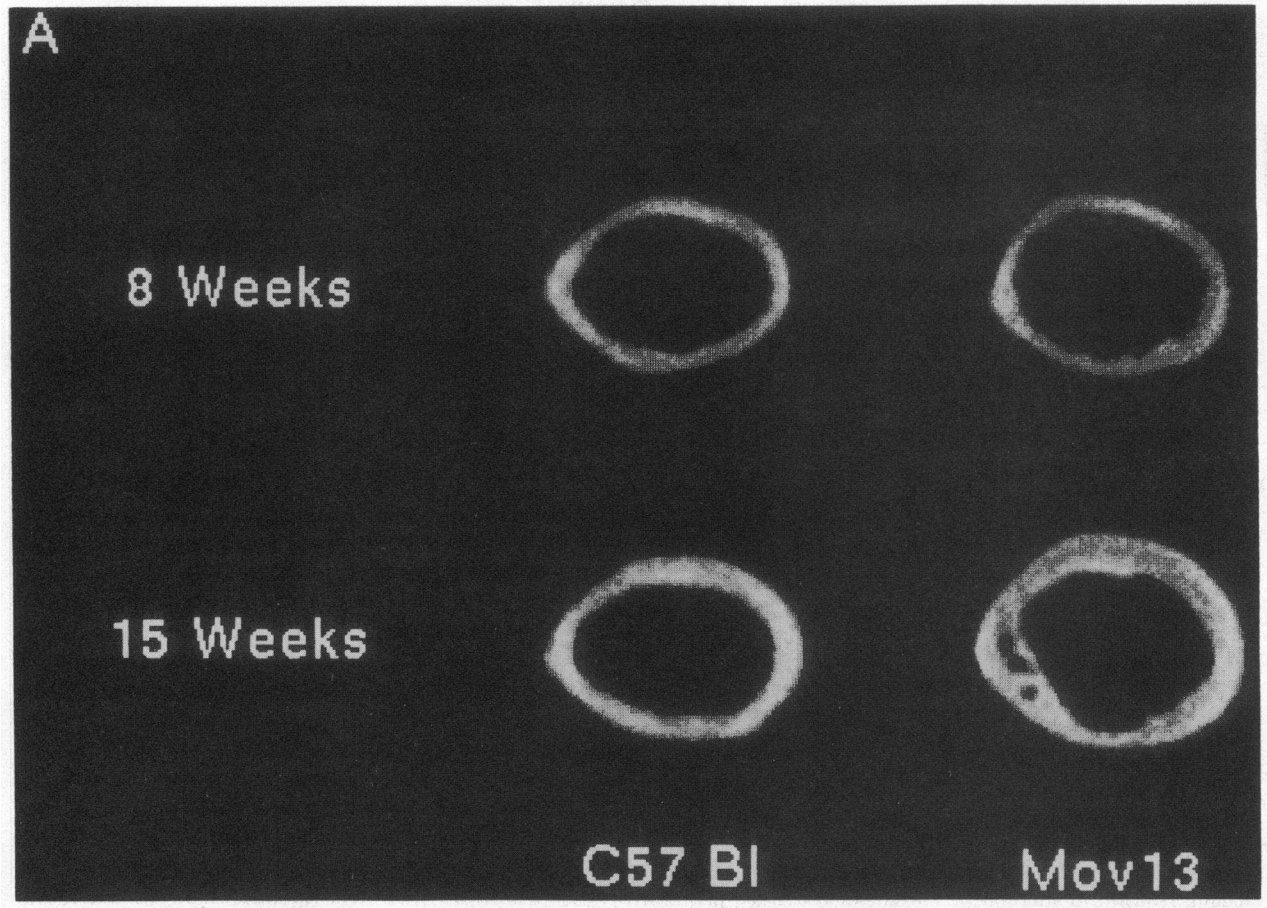
A
8 Weeks
15 Weeks
C57 Bl
Mov13

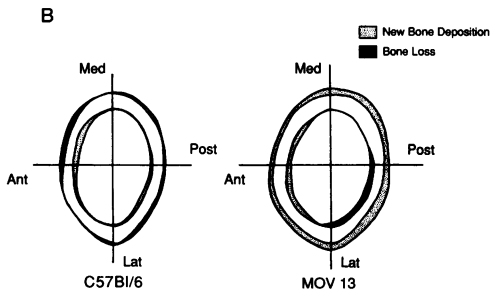
B
New Bone Deposition
Bone Loss
Med
Post
Ant
Lat
C57Bl/6
Med
Post
Ant
Lat
MOV 13

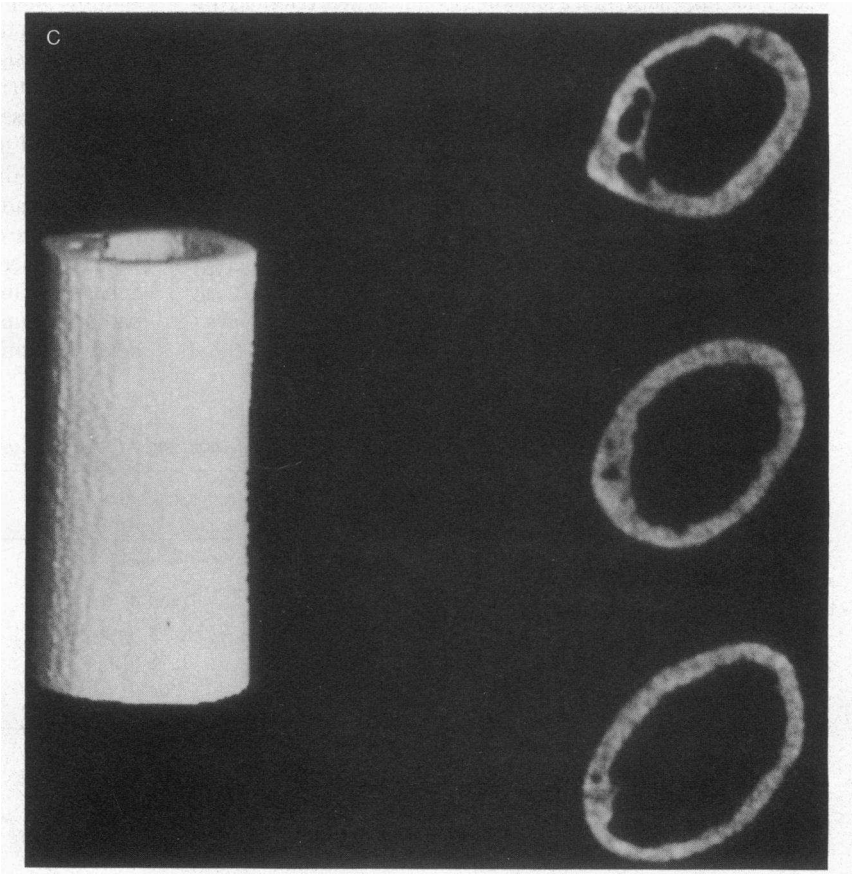
C

Table III. Geometrical Properties (Cross-sectional Radius) of (C57 BI/6) Wild-type and Mov13 Specimens

Mouse	Age	r_{AP}	r_{ML}	Measured Failure Load	Predicted Failure Load
	wk	*mm*	*mm*	*(N)*	*(N)*
C57 BI/6	8	0.64 (0.03)	0.91 (0.04)	21.2 (4.9)	21.5
Mov13	8	0.66 (0.04)	0.91 (0.04)	19.7 (4.0)	23.4
C57 BI/6	15	0.61 (0.04)	0.93 (0.06)	25.5 (5.4)	21.7
Mov13	15	0.70 (0.02)*‡	0.99 (0.06)‡	31.6 (6.6)§	31.0

Properties were calculated as described in Methods. r_{AP} is the radius along the Anterior-Posterior axis. r_{ML} is the radius along the Medial-Lateral axis.

* Comparison between Mov13 and C57 BI/6 at 15 wk, $P < 0.001$.

‡ Comparison between Mov13 at 8 and 15 wk $P < 0.02$.

§ Comparison between Mov13 at 8 and 15 wk $P < 0.005$.

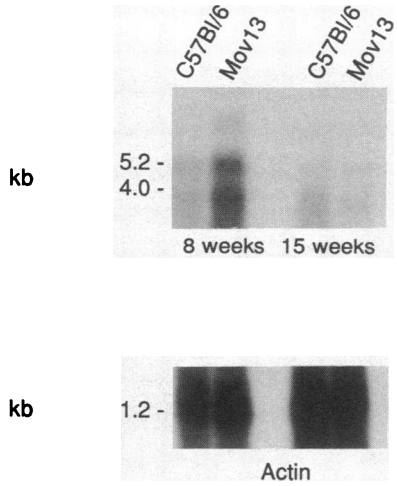

Figure 3. Type I collagen mRNA expression. Total RNA was prepared separately from the femurs of 8- and 15-wk wild-type (C57 BI/6) and Mov13 mice by as described under Methods. As expected (16) the $\alpha 1$(I) collagen probe hybridized to two mRNA species of ~ 4.0 and 5.2 kb. Preliminary studies with independent specimens from a total of eight transgenic and control mice established a direct correlation between the number of whole femur specimens and the amount of steady-state β-actin mRNA (data not shown).

image of 8- and 15-wk wild-type specimens was essentially unchanged because the gain and loss of bone over time were essentially unchanged. In contrast, a net increase in the area of Mov13 cortical bone was due for the most part from new bone deposition along the periosteal surface. The deposition of new bone increased the cross-sectional radius of the mid-diaphysis of Mov13 specimens by ~ 8% (Table III).

The observed relationship between cross-sectional radius and the failure load of endochondral bone agrees with a large body of descriptive, experimental, and analytical work investigating the relationship between the shape and strength of objects such as long bone. We compared the predicted and observed failure load values for wild-type and Mov13 specimens to estimate what portion of the age-related increase in Mov13 whole bone bending load could be attributed solely to the increase in cross-sectional area. Failure load was predicted using a typical "strength of materials" approach (20),

$$\sigma = Mc/I$$

where σ is the bending strength of the cortical tissue, M is moment at failure from which the failure load can be derived, c is the distance from the periosteal surface to the geometric centroid (assuming failure in tension), and I is the bending moment of inertia. Since our goal was to determine the influence of the change in geometric properties independent of any change in material properties, we assumed that all specimens had the same tissue bending strength of 120 MPa. For the given age-related increase in Mov13 cross-sectional area, we predicted a 33% increase in whole bone failure load. This result agreed quite well with the results shown in Fig. 2 and Tables II and III. Thus, for an ~ 8% increase in the cross-sectional radius of Mov13 cortical bone, a 37.7% increase in the failure load was obtained.

Type I collagen is the most abundant constituent in bone, and the molecule has a prominent role in bone adaptation, remodeling, and repair. To evaluate potential alterations in type I collagen gene expression that may have occurred as Mov13 specimen geometry increased, mRNA was obtained from whole femurs of Mov13 and wild-type mice at 8 and 15 wk of age. Steady-state mRNA levels for the $\alpha 1$(I) collagen chain were evaluated by Northern blotting (Fig. 3). As expected (16), the signals from wild-type specimens at both 8 and 15 wk were relatively small. In contrast, the level of collagen expression in Mov13 specimens at 8 wk was significantly increased (~ 30% by scanning gel densitometry, data not shown) compared with wild-type. Expression then decreased to a level similar to wild-type by 15 wk. Thus, an increase in Mov13 $\alpha 1$(I) collagen mRNA expression antedated the increase in cortical bone geometrical properties.

We next sought to determine if the increase in Mov13 collagen mRNA at 8 wk was associated with an increase in bone cell number, as seemed likely given the nature of the Mov13 mutation. We ascertained cell number using stereological techniques and SEM of a group of wild-type and Mov13 mid-diaphyseal specimens. As shown in Fig. 4, we observed a significant increase ($P < 0.0001$) in the number of Mov13 bone cell lacunae per mm^3. Thus, the increase in mRNA appears to result at least in part from a cellular proliferative process.

Finally, we sought to identify alterations in mineral content that may have accompanied the change in geometry (Fig. 5). The amount of bone and mineral per unit volume and the mineral/matrix ratio remained essentially constant in 8- and 15-wk wild-type specimens. Consistent with the proposed effect of the Mov13 mutation, the amounts of mineral and of matrix per unit volume decreased significantly in the 8-wk specimens (Fig. 5, *A* and *B*). As the cross-sectional geometry increased, however, both parameters increased to near wild-type levels. In contrast, the ratio of mineral to matrix remained constant in the 8- and 15-wk Mov13 specimens (Fig. 5 *C*).

Figure 2. Whole bone geometry. Geometrical properties were derived from micro-computed tomography studies as described in Methods. (*A*) Representative transverse sections of the micro-computed tomography analysis. (*B*) Superimposition of representative 8- and 15-wk cross-sectional images. (*C*) Entire reconstruction of the mid-diaphysis of a typical Mov13 femur specimen. Cross sections from the upper, middle, and lower portions of the reconstructed image are shown at the right. Note that 1 mm of the image = 0.54 mm of the actual specimen.

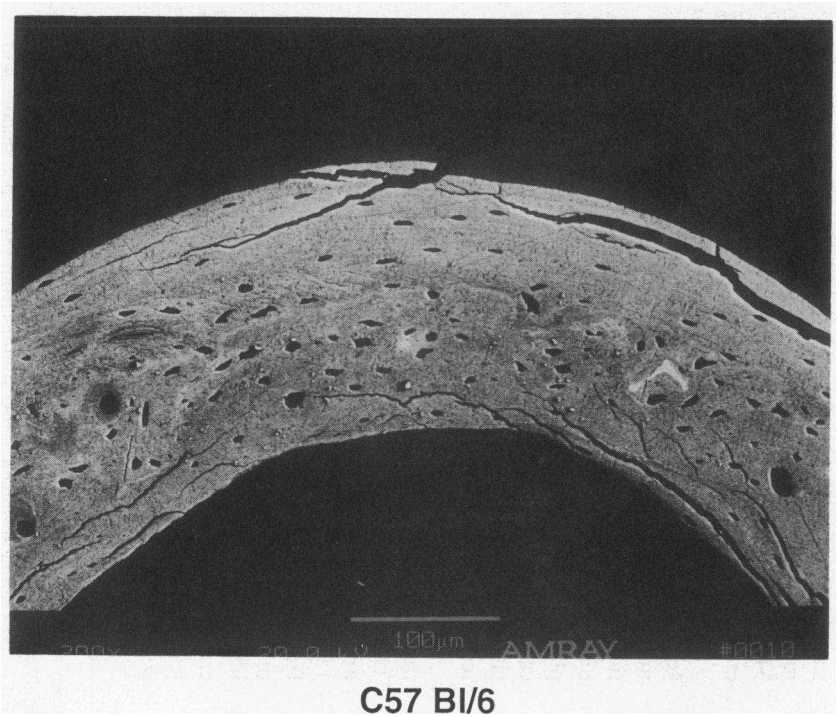
C57 Bl/6

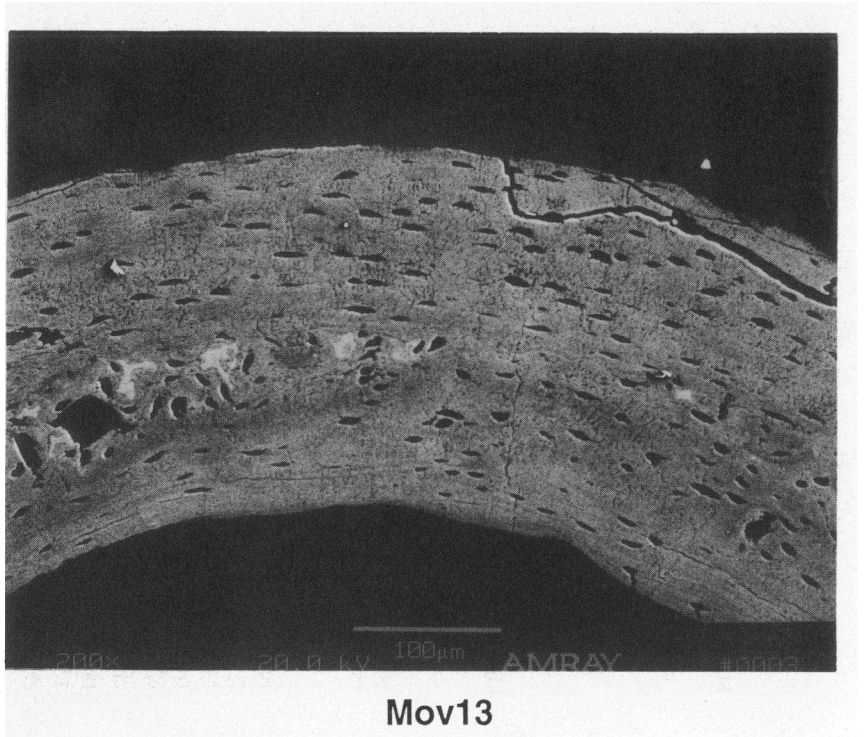
Mov13

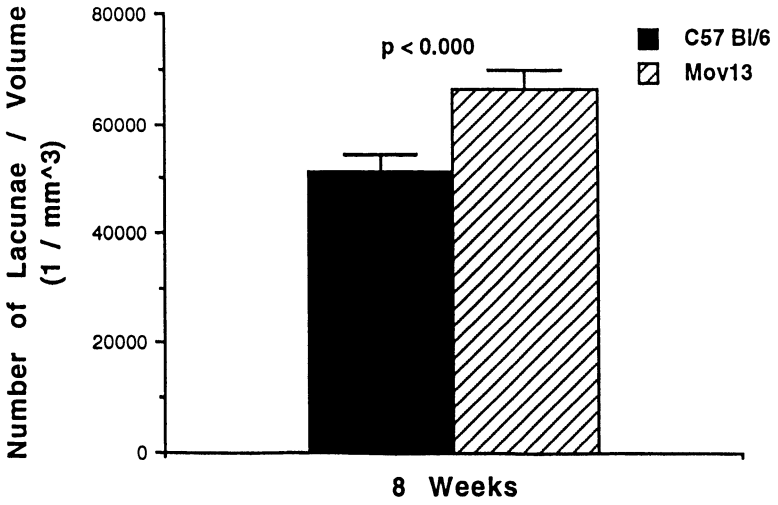
Number of Lacunae / Volume (1 / mm^3)
80000
60000
40000
20000
0
p < 0.000
C57 Bl/6
Mov13
8 Weeks

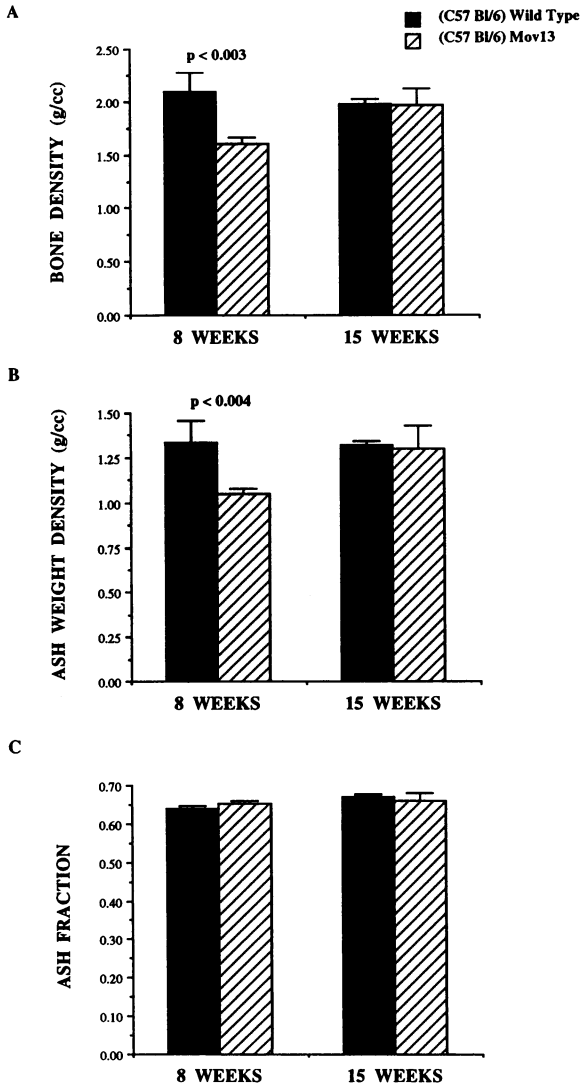

Figure 5. Bone mineralization. Mineralization was evaluated as described in Methods.

Discussion

Remarkable progress has been made in understanding the molecular basis of osteogenesis imperfecta. Presently, more than 100 mutations have been characterized at the sequence level. This effort has firmly established the association between dominantly inherited mutations in type I collagen genes and all clinical forms of osteogenesis imperfecta (4). Both null and structural mutations have been reported, and null mutations in particular are linked to OI type I. Despite this wealth of sequence information, the tissue pathogenesis of OI is not well understood. A long-term goal of our Mov13 studies is to determine how a heterozygous null α1(I) collagen allele results in skeletal fragility. The principal advantages of a mouse model are that the mutation can be studied on a single genetic background and that the effect of the mutation can be evaluated using syngeneic littermates as controls. Our studies to date have shown that the Mov13 mutation disrupts both the ductility and strength of long bones (as measured by a decrease in plastic deformation and a decrease in failure load, respectively). Consequently, skeletal tissues lose some of their toughness or durability as their collagen content decreases. It follows from these observations that the long bones of Mov13 mice will "wear out" more quickly under repetitive loading conditions. We are testing this hypothesis by conducting fatigue tests on Mov13 whole bone specimens and microspecimens.

Why does the Mov13 mutation have a dominant effect on bone mechanical integrity? Bone tissue consists of about a dozen proteins, which are assembled with precision in time and space to form a highly ordered extracellular matrix (21). Type I collagen contributes to the load-bearing capacity of the skeleton by assembling into ordered fibrils that associate with plate-shaped crystals of carbonate apatite and with other extracellular matrix molecules. As demonstrated previously in yeast (22), the function of highly ordered, multimeric protein complexes can be disrupted by genetic alterations in the amount of one component molecule. We have hypothesized that the heterozygous Mov13 mutation alters the relative amount of type I collagen in bone extracellular matrix and thus, in a dominant manner, is able to alter properties such as the plastic deformation of whole bones (12). This alteration in properties apparently predisposes bone tissue to fail as it is repetitively loaded.

This study describes a skeletal adaptation in Mov13 mice that occurs without any experimental manipulation. The Northern and histomorphometric analyses demonstrated an 8% increase in the cross section of Mov13 femurs that was mediated for the most part by periosteal bone cells. The adaptive response occurred over a 2-mo period, during which time a small number of newly proliferated osteogenic cells produced a small amount of new bone along periosteal surfaces. Previous studies have indicated that the geometric redistribution of bone tissue is an important means of preserving bone strength and rigidity under conditions of decreasing bone quality (23–26). Moreover, age-related geometrical remodeling of the skeleton appears to be a characteristic of both trabecular (27, 28) and cortical bone (29–31), and may be a feature of disease processes such as osteoporosis (32). The results of this study extend these observations to heritable diseases associated with skeletal fragility such as osteogenesis imperfecta type I. To the best of our knowledge, this work is the first evidence that the geometry/strength paradigm is valid for osteogenesis imperfecta bone.

The natural history of OI type I is somewhat puzzling in that the fracture frequency of affected individuals often decreases dramatically at puberty while other aspects of phenotype (e.g., hearing loss) progressively worsen with age (33). To explain the striking decrease in fracture frequency, some investigators have noted that bone mineral content normally increases at puberty, suggesting that the increase in mineral accounts for the decreased fracture rate (34). However, the pro-

Figure 4. Bone cell lacunar density. Scanning electron microscopy and the stereological analysis were performed as described under Methods. Representative photographs taken from the medial quadrant of the femoral mid-diaphysis are shown. Specimen cracks are an artifact of specimen handling. Bar (2 mm), 100 μm.

pensity of long bone to fracture is determined by several factors besides mineral content. These factors include the loading history as well as the structural, material, and fatigue properties of bone, which are determined by the quality and quantity of the matrix, the quality and quantity of the mineral, and interactions between these two tissue compartments as the bone is loaded. It is unlikely, therefore, that an increase in mineral content alone could completely explain the dramatic decrease in the fracture rate of individuals with OI type I. Given the large body of evidence, which indicates that biomineralization is a highly regulated process and that the mineral/matrix ratio is maintained as a constant in normal vertebrate bone (3), it also seems unlikely that the ratio of mineral to matrix in human bone actually changes significantly at puberty. Along this line, a disproportionate increase in mineral actually could have a deleterious effect on mechanical integrity by making bone tissue more brittle than normal; i.e., the relative increase in mineral content could be associated with a high apparent modulus value but a low value of fracture toughness due to the reduced capability of bone to stop crack propagation as the volume fraction of mineral increases (35–37).

The Mov13 adaptation suggests an alternative explanation for the decreased fracture frequency of individuals with OI at puberty. The explanation is based on the unique and often dramatic change in the structure of the skeleton that occurs at this time, i.e., the growth spurt. Bone growth involves a complex set of processes that occur throughout the life of an individual. This process begins during prenatal life and continues until, in the case of endochondral bone, the epiphysis closes and bone growth ceases. Previous studies have shown that the growth spurt alters the length as well as width of long bone (38). Indeed, it can be argued that this must be the case based on established structure–function relationships. As long bones grow, they tend to lose compressive strength if they maintain the original proportion of shaft length to shaft cross-section (39), an effect that becomes more pronounced as growth increases. Therefore, to maintain comparable strength, long bones normally become disproportionately thicker relative to length as they grow. These considerations lead us to suggest that as individuals with OI type I undergo the growth spurt at puberty, changes in the cross-sectional geometry of their long bones compensate the effect of their collagen gene mutation and, consequently, modify their OI type I phenotype.

The Mov13 adaptation suggests a general strategy to make weak bone stronger. The cellular target of this strategy is the osteoblast on the periosteal surface of bone. The goal is to induce these cells to synthesize, deposit, and mineralize new bone matrix, thereby increasing the cross-sectional radius. This strategy could be implemented by (*a*) increasing bone cell number but keeping the metabolic activity per cell a constant; (*b*) keeping bone cell number a constant but increasing the metabolic activity of each cell; or (*c*) both. The prediction is that small increases in cross-section will significantly increase the mechanical properties of bone. A principal goal of our future studies will be to identify anabolic agents that stimulate periosteal new bone formation. An alternative is to identify a gene or group of genes that, when overexpressed, achieve the same effect. The goal of these efforts is to decrease the fracture rate of individuals with heritable, and perhaps other, forms of skeletal fragility.

Acknowledgments

The authors are grateful to M. Brown for assistance with the statistical analyses and to R. Curry for animal care and production.

These studies were supported in part by the National Institutes of Health (AR40679, AR20557) and by a National Science Foundation Graduate Research Fellowship (M. K. Mansoura).

References

1. Swanson, S. A., M. A. R. Freeman, and W. H. Day. 1971. *Med. Biol. Eng.* 9:23–32.

2. Martin, R. B., and D. B. Burr. 1984. Structure, Function, and Adaptation of Compact Bone. Raven Press, New York. 275 pp.

3. Lowenstam, H. A., and S. Weiner. 1989. On Biomineralization. Oxford University Press, New York. 324 pp.

4. Bonadio, J., and S. A. Goldstein. Our understanding of inherited skeletal fragility and what this has taught us about bone structure and function. *In* Molecular Biology of Bone. G. Noda, editor. Academic Press, Orlando, FL. In press.

5. Schnieke, A., K. Harbers, and R. Jaenisch. 1983. Embryonic lethal mutation in mice induced by retrovirus insertion into the α1(I) collagen gene. *Nature (Lond.)*. 304:315–320.

6. Harbers, K., M. Kuehn, H. Delius, and R. Jaenisch. 1984. Insertion of retrovirus into first intron of α1(I) collagen gene leads to embryonic lethal mutation in mice. *Proc. Natl. Acad. Sci. USA*. 81:1504–1508.

7. Kratochwil K., K. von der Mark, E. J. Kollar, R. Jaenisch, K. Mooslehner, M. Schwarz, K. Haase, I. Gmachl, and K. Harbers. 1989. Retrovirus-induced insertional mutation in Mov13 mice affects collagen I expression in a tissue-specific manner. *Cell*. 57:807–816.

8. Schwarz, M., K. Harbers, and K. Kratochwil. 1990. Transcription of a mutant collagen I gene is a cell type and stage-specific marker for odontoblast and osteoblast differentiation. *Development (Camb.)*. 108:717–726.

9. Lohler, J., R. Timpl, and R. Jaenisch. 1984. Embryonic lethal mutation in mouse collagen I gene causes rupture of blood vessels and is associated with erythropoietic and mesenchymal cell death. *Cell*. 38:597–607.

10. Dziadek, M., R. Timpl, and R. Jaenisch. 1987. Collagen synthesis by cell lines derived from Mov13 mouse embryos which have a lethal mutation in the collagen α1(I) gene. *Biochem. J.* 244:375–379.

11. Bonadio, J., T. L. Saunders, E. Tsai, S. A. Goldstein, J. Morris-Wiman, L. Brinkley, D. F. Dolan, R. A. Altschuler, J. E. Hawkins, J. F. Bateman, et al. 1990. A transgenic mouse model of osteogenesis imperfecta type I. *Proc. Natl. Acad. Sci. USA*. 87:7145–7149.

12. Jepsen, K., Mansoura, M., Kuhn, J. L., Jaenisch, R., Bonadio, J., and S. A. Goldstein. 1992. An in vivo assessment of the contribution of type I collagen to the mechanical properties of cortical bone. *Orthop. Trans.* 17:93.

13. Feldkamp, L. A., and G. Jesion. 1986. 3-D x-ray computed tomography. *In* Review of Progress in Quantitative Nondestructive Evaluation. D. E. Chimenti, editor. Vol. 5A. Plenum Press, New York. 555–566.

14. Kuhn, J. L., S. A. Goldstein, L. A. Feldkamp, R. Goulet, and G. Jesion. 1990. Evaluation of a microcomputed tomography system to study trabecular bone structure. *J. Orthop. Res.* 8:833–842.

15. Wong, M., T. Lawton, P. F. Goetinck, J. L. Kuhn, S. A. Goldstein, and J. Bonadio. 1992. Aggrecan core protein is expressed in membranous bone of the chick embryo. *J. Biol. Chem.* 267:5592–5598.

16. Mooslehner, K., and K. Harbers. 1988. Two mRNAs of the mouse pro α1 (I) collagen gene differ in the size of the 3'-untranslated region. *Nucleic Acids Res.* 16:773.

17. Kost, T. A., N. Theodorakis, and S. H. Hughes. The nucleotide sequence of the chick cytoplasmic β-actin gene. 1983. *Nucleic Acids Res.* 11:8287–8301.

18. Sissons, H. A., and P. O. O'Connor. 1977. Quantitative histology of osteocyte lacunae in normal human cortical bone. *Calcif. Tissue Res.* 22:530–533.

19. Carter, D. R., and W. C. Hayes. 1977. The compressive behavior of bone as a two-phase porous structure. *J. Bone Jt. Surg. Am. Vol.* 59:954–962.

20. Beer, F. P., and E. R. Johnston. 1981. Mechanics of Materials. McGraw Hill Co., New York. 616 pp.

21. Robey, P. G. 1989. Metabolic bone disease. *Endocrinol. Metab. Clin. North Am.* 18:859–902.

22. Meeks-Wagner, D., and L. H. Hartwell. 1986. Normal stoichiometry of histone dimer sets is necessary for high fidelity of mitotic chromosome transmission. *Cell*. 44:43–52.

23. Fung, Y. C. 1981. Biomechanics: Mechanical Properties of Living Tissues. Springer-Verlag New York Inc., New York. 433 pp.

24. Ruff, C. B., and W. C. Hayes. 1988. Sex differences in age-related remodeling of the femur and tibia. *J. Orthop. Res.* 6:886–896.

25. Jones H. H., J. D. Priest, W. C. Hayes, C. C. Tichenor, and D. A. Nagel. 1977. Humeral hypertrophy in response to exercise. *J. Bone Jt. Surg. Am. Vol.* 59A:204–208.

26. Lanyon, L. E. 1982. Mechanical function in bone remodeling. *In* Bone in Clinical Orthopaedics. G. Sumner Smith, editor. W. B. Saunders Co., Philadelphia. 273–304.

27. Woo, S. L. Y., S. C. Kuei, D. Amiel, M. A. Gomez, W. C. Hayes, F. C. White, and W. H. Akeson. 1981. The effect of prolonged physical training on the properties of long bone: a study of Wolff's law. *J. Bone Jt. Surg. Am. Vol.* 63A:780–787.

28. Kerr, R., D. Resnick, D. J. Sartoris, S. Kursunoglu, C. Pineda, P. Haghghi, G. Greenway, and J. Guerra, Jr. 1986. Computerized tomography of proximal femoral trabecular patterns. *J. Orthop. Res.* 4:45–56.

29. Kleerekoper, M., A. R. Villananueva, J. Stanciu, D. S. Rao, and A. M. Parfitt. 1985. The role of three-dimensional trabecular microstructure in the pathogenesis of vertebral compression fractures. *Calcif. Tissue Int.* 37:594–597.

30. Garn, S. M. 1970. The Earlier Gain and the Later Loss of Cortical Bone. Charles C. Thomas, Springfield, IL. 146 pp.

31. Ruff, C. B., and W. C. Hayes. 1982. Subperiosteal expansion and cortical remodeling of the human femur and tibia with aging. *Science (Wash. DC).* 217:945–948.

32. Martin, R. B., and Atkinson, P. J. 1977. Age and sex-related changes in the structure and strength of the human femoral shaft. *J. Biomech.* 10:233–241.

33. Paterson, C. R., S. McAllion, and J. L. Stellman. 1984. Osteogenesis imperfecta after the menopause. *N. Engl. J. Med.* 310:1694–1969.

34. Smith, R., M. J. O. Francis, and G. R. Houghtin. 1983. The Brittle Bone Syndrome: Osteogenesis Imperfecta. Butterworths, London. 218 pp.

35. Ascenzi, A., and E. Bonucci. 1967. The tensile properties of single osteons. *Anat. Rec.* 158:375–385.

36. Ascenzi, A., and E. Bonucci. 1968. The compressive properties of single osteons. *Anat. Rec.* 161:377–391.

37. Currey, J. D. 1969. The mechanical consequences of variation in the mineral content of bone. *J. Biomech.* 2:1–11.

38. Shipman, P., A. Walker, and D. Bichell. 1985. Bone growth. *In* The Human Skeleton. Harvard University Press, Cambridge, MA. 38–49.

39. Currey, J. D. 1984. The Mechanical Adaptations of Bone. Princeton University Press, Princeton, NJ. 294 pp.